

The BeppoSAX High Energy Large Area Survey HELLAS, III: testing synthesis models for the X-ray background

A. Comastri¹, F. Fiore^{2,3}, C. Vignali^{1,4}, G. Matt⁵, G.C. Perola⁵, F. La Franca⁵

¹ *Osservatorio Astronomico di Bologna, via Ranzani 1, I-40127 Bologna, Italy*

² *Osservatorio Astronomico di Roma, Via Frascati 33, I-00044 Monteporzio, Italy*

³ *BeppoSAX Science Data Center, Via Corcolle 19, I-00131 Roma, Italy*

⁴ *Dipartimento di Astronomia, Università di Bologna, via Ranzani 1, I-40127 Bologna, Italy*

⁵ *Dipartimento di Fisica, Università degli Studi “Roma Tre”, Via della Vasca Navale 84, I-00146 Roma, Italy*

26 April 2024

ABSTRACT

The BeppoSAX High Energy Large Area Survey (HELLAS) has surveyed several tens of square degrees of the sky in the 5–10 keV band down to a flux of about 5×10^{-14} erg cm⁻² s⁻¹. The source surface density of 16.9 ± 6.4 deg⁻² at the survey limit corresponds to a resolved fraction of the 5–10 keV X-ray background (XRB) of the order of 20–30 %. The extrapolation of the HELLAS logN–logS towards fainter fluxes with an euclidean slope is consistent with the first XMM–*Newton* measurements, in the same energy band, which are a factor 20 more sensitive. The source counts in the hardest band so far surveyed by X-ray satellites are used to constrain XRB models. It is shown that in order to reproduce the 5–10 keV counts over the range of fluxes covered by BeppoSAX and XMM–*Newton* a large fraction of highly absorbed ($\log N_H = 23$ – 24 cm⁻²), luminous ($L_X > 10^{44}$ erg s⁻¹) AGN is needed. A sizeable number of more heavily obscured, Compton thick, objects cannot be ruled out but it is not required by the present data. The model predicts an absorption distribution consistent with that found from the hardness ratios analysis of the so far identified HELLAS sources. Interestingly enough, there is evidence of a decoupling between X-ray absorption and optical reddening indicators especially at high redshifts/luminosities where several broad line quasars show hardness ratios typical of absorbed power law models with $\log N_H = 22$ – 24 cm⁻².

Key words: X-ray: background – galaxies – AGN

1 INTRODUCTION

Hard X-ray surveys can permit to resolve directly the sources making the hard Cosmic X-ray background (XRB) and so provide strong constraints on unification schemes and AGN synthesis models for the XRB. According to these models a large fraction of the 2–100 keV XRB energy density is due to obscured AGN (Setti & Woltjer 1989; Madau, Ghisellini & Fabian 1994; Comastri et al. 1995; Gilli, Risaliti & Salvati 1999; Wilman & Fabian 1999; Pompilio, La Franca & Matt 2000), emerging at high energies. A major step forward in the study of the hard X-ray sky has been achieved by ASCA (Georgantopoulos et al. 1997; Cagnoni Della Ceca, Maccacaro 1998; Boyle et al. 1998; Ueda et al. 1998, 1999; Della Ceca et al. 1999) and BeppoSAX (Giommi Perri & Fiore 2000). At the flux limit of the deepest ASCA and BeppoSAX surveys in the 2–10 keV band ($\sim 5 \times 10^{-14}$ erg cm⁻² s⁻¹) about 30 % of the XRB is resolved into single sources. *Chandra* and XMM–*Newton* pushed the 2–10

keV flux limit ≈ 20 times fainter, resolving between 70 and 100 % of the hard X-ray Cosmic background (Mushotzky et al. 2000, Giacconi et al. 2001; Hasinger et al. 2001). Optical follow-up observations (Akiyama et al. 2000; Fiore et al. 1999, 2000; Mushotzky et al. 2000; Giacconi et al. 2001), revealed that a large fraction of these sources are AGN and that a sizeable fraction of them show evidence of X-ray and optical obscuration. Absorbed AGN can be detected, of course less efficiently, also below 2 keV. Indeed, the optical identification process of deep and ultra-deep ROSAT PSPC and HRI surveys (resolving $\sim 70\%$ of the 0.5–2.0 keV XRB, Hasinger et al. 1998), finds that about one fourth of the sources are intermediate AGN or narrow line galaxies, likely sites of high obscuration (the remaining sources being broad line quasars, Schmidt et al. 1998, Lehmann et al. 2000).

In order to investigate the nature of the sources of the hard XRB we have carried out a systematic search of X-ray

sources in the 5–10 keV energy range, the hardest band accessible with imaging instruments. The High Energy Large Area Survey (HELLAS) is described in detail by Fiore et al. (2001, paper II). The hard X-ray selected sources have been extensively observed also at other wavelengths. The results of optical identifications are reported by Fiore et al. (1999, paper I) and La Franca et al. (in preparation, paper V); the search for soft X-ray counterparts in the ROSAT PSPC archive is reported by Vignali et al. (2001, paper IV), while the results of VLA radio observations are discussed by Ciliegi et al. (in preparation, paper VI). Here we show that the BeppoSAX and XMM-*Newton* source counts in the 5–10 keV energy range and the average spectral properties of HELLAS sources provide further constraints on the absorption and luminosity distribution of the sources making the hard XRB and on AGN synthesis models. We also show the need of a large number of highly obscured ($\log N_H = 23\text{--}24 \text{ cm}^{-2}$), high luminosity sources to reproduce the XRB spectrum and the number counts. $H_0 = 50 \text{ km s}^{-1} \text{ Mpc}^{-1}$ and $q_0 = 0$ are adopted throughout this paper.

2 THE BEPPoSAX HELLAS SURVEY

The survey is presented in the companion paper by Fiore et al. (paper II). Briefly, the High Energy Large Area Survey (HELLAS) covers about 85 square degrees in the 5–10 keV band down to a flux limit of $\sim 5 \times 10^{-14} \text{ erg cm}^{-2} \text{ s}^{-1}$. Sources were detected and characterized statistically using the methods described in the companion paper. The quality of the detection has always been checked interactively. The count rates were converted to fluxes using a fixed conversion factor equal to $7.8 \times 10^{-11} \text{ erg cm}^{-2} \text{ s}^{-1}$ (5–10 keV flux) per one “3 MECS count” (4.5–10 keV). Due to the narrowness of the band this factor is not strongly sensitive to the actual spectral shape. The sample used for computing the logN-logS includes 147 sources. Optical identifications are available for about one third of the sample (La Franca et al. 2000).

3 THE XRB MODEL

The increasing amount of observational data concerning both the XRB spectral intensity and the source counts in several energy ranges obtained by ROSAT, ASCA and BeppoSAX surveys coupled with the optical identification of sizeable samples of hard X-ray selected sources (Fiore et al. 1999, 2000, Akiyama et al. 2000) have revived the interest on AGN synthesis models for the XRB (Gilli et al. 1999; Wilman & Fabian 1999; Pompilio et al. 2000). A detailed treatment of XRB synthesis models using the most recent observational constraints, including the AGN luminosity function derived from ROSAT deep surveys (Miyaji et al. 2000) and the column density distribution of Seyfert 2 galaxies in the local Universe estimated by Risaliti et al. (1999), is extensively discussed by Gilli et al. (2001), while a comparison between the different approaches is reviewed by Comastri (2000). Even though a large fraction of the XRB spectral intensity and the source counts are fairly well reproduced by AGN synthesis models, a self-consistent description of the XRB constituents has yet to be reached as

most of its ingredients have to be extrapolated well beyond the present observational limits.

In almost all the AGN synthesis models for the XRB it is assumed that the space density and evolution of the unabsorbed population can be modeled by the QSO X-ray luminosity function computed from ROSAT surveys (Boyle et al. 1993, 1994; Miyaji et al. 2000). Obscured sources are then added with a distribution of column densities and with the further assumption that their luminosity function and evolution are the same of unobscured population. Even though this approach seems reasonable, it is however plausible that absorbed objects could slip into deep ROSAT surveys at faint fluxes and thus skew the interpretation of the luminosity function and the modelling of the XRB. The possible “contamination” of absorbed objects is minimized using the luminosity function parameters obtained from relatively shallow ROSAT surveys above $\sim 10^{-14} \text{ erg cm}^{-2} \text{ s}^{-1}$ in the 0.5–2 keV band (Boyle et al. 1993, 1994) which are essentially dominated by unabsorbed objects (see also Fig. 4a). The lack of a trend for a change in hardness ratio with redshift (Almaini et al. 1996) adds further weight to the assumption that this is a fair “unobscured” sample.

For the purpose of the present paper we adopt the Comastri et al. (1995 hereinafter C95) model with a few variations and improvements and test its prediction against the HELLAS and XMM *Newton* survey findings. With respect to C95 the spectrum of heavily absorbed AGN ($\log N_H > 24$) is now computed taking into account Compton scattering effects by means of a Montecarlo code (Matt, Pompilio & La Franca 1999). The luminosity evolution, parameterized with a power law model $L(z) = L(z=0) \times (1+z)^{2.6}$, stops at $z_{cut} = 1.8$ and then stays constant up to $z_{max} = 3$. The shape and normalization of the luminosity function are slightly different from those adopted in C95 and consistent with the values of Boyle et al. (1994). The choice of these parameters is consistent with the more recent estimates of the high redshift AGN evolution and also fits well the first *Chandra* measurements. A more detailed comparison with observational data will be discussed in the following section(s).

The input AGN spectra, including the subdivision in the N_H classes centered at $\log N_H = 21.5, 22.5, 23.5, 24.5$, are as described in C95, while the best fit absorption distribution of obscured AGN in the four N_H classes normalized to the space density of unobscured AGN, turned out to be 0.35, 1.5, 2.3, 2.0 which is slightly different from that reported by C95 for two reasons. The first is that some input parameters have been changed as described in the previous paragraph, the second concerns the intensity of the 1–8 keV XRB spectrum which has to be fitted by the model. The ASCA (Gendreau et al. 1995) and BeppoSAX (Vecchi et al. 1999) observations of the XRB spectrum below 8 keV are significantly higher than the average level measured by HEAO1–A2 (Marshall et al. 1980). The maximum discrepancy is between the BeppoSAX and HEAO1–A2 observations, the level of the latter being lower by 30–40 % in the overlapping 3–8 keV band. The best fit ASCA spectrum lies approximately in between and thus we choose to fit the XRB spectral intensity as measured by ASCA.

The best fit absorption distribution is compared with that derived by Risaliti et al. (1999) in Fig. 1. Even though the relative fraction of objects in the various N_H bins is

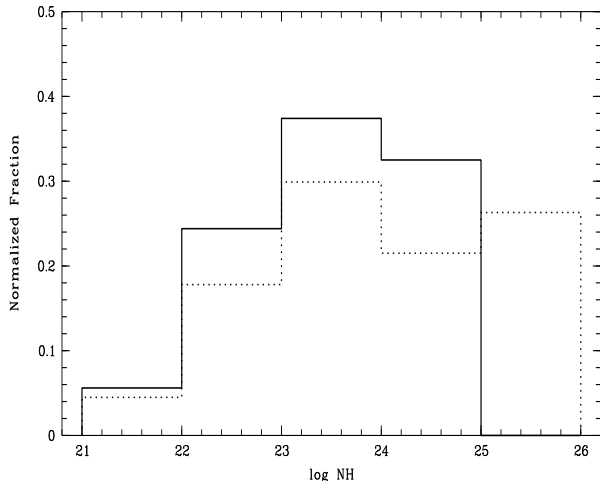


Figure 1. The model absorption distribution (solid line) compared with the observed N_H distribution for a sample of nearby Seyfert 2 galaxies (Risaliti et al. 1999). The two histogram are renormalized to the same ratio between obscured and unobscured objects.

different the overall shape of the two distributions is similar. The peak in both cases is in the $\log N_H = 23$ –24 bin and a large fraction of the objects (70–80 %) is obscured by column densities greater than 10^{23} cm^{-2} . As a consequence the large fraction of highly obscured objects needed to fit the XRB spectral intensity is consistent with the absorption distribution of Seyfert 2 galaxies in the local Universe.

Sources with column densities in excess of 10^{25} cm^{-2} are not included in the present model as their contribution to the XRB is never energetically relevant (see e.g. Gilli et al. 1999) even if they could constitute a sizeable fraction of the obscured AGN population (Risaliti et al. 1999).

4 THE INTEGRAL LOGN-LOGS COMPARED WITH MODEL PREDICTIONS

Figure 2 presents the integral 5–10 keV $\log N$ – $\log S$ of the 147 HELLAS sources. The $\log N$ – $\log S$ can be represented by a power law model $N(> S) = KS^{-q}$ below a flux of $4 \times 10^{-13} \text{ erg cm}^{-2} \text{ s}^{-1}$. The best fit power law index is $q = 1.56 \pm 0.14(0.34)$. Errors represent the 90 % confidence interval, errors in brackets include systematic uncertainties. The normalization K of the best fit power law at $10^{-13} \text{ erg cm}^{-2} \text{ s}^{-1}$ is 5.24 deg^{-2} . Above $\sim 4 \times 10^{-13} \text{ erg cm}^{-2} \text{ s}^{-1}$ the $\log N$ – $\log S$ steepens significantly. This is probably due to a selection effect. The probability to find a bright source near a, usually, bright target is small, and therefore the number of bright sources in a serendipity survey like the HELLAS survey tends to be underestimated. The derived shape of the $\log N$ – $\log S$ may be affected by several biases which are extensively discussed in paper II. For the purposes of the present discussion we compare the model predictions with the best estimate of HELLAS counts taking into account both statistical and systematic errors.

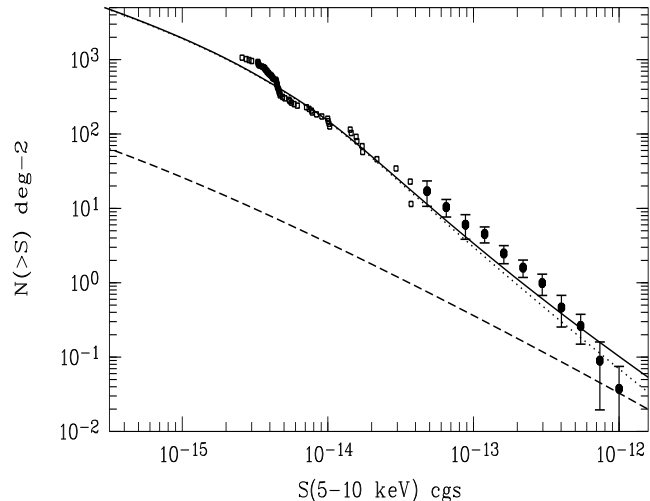


Figure 2. The 5–10 keV integral $\log N$ – $\log S$ as measured by BeppoSAX (filled circles with error bars) and XMM–Newton (open squares). Thick line = total (AGN+clusters) 5–10 keV counts predicted by the XRB synthesis model; dotted line = AGN only; dashed line = clusters only.

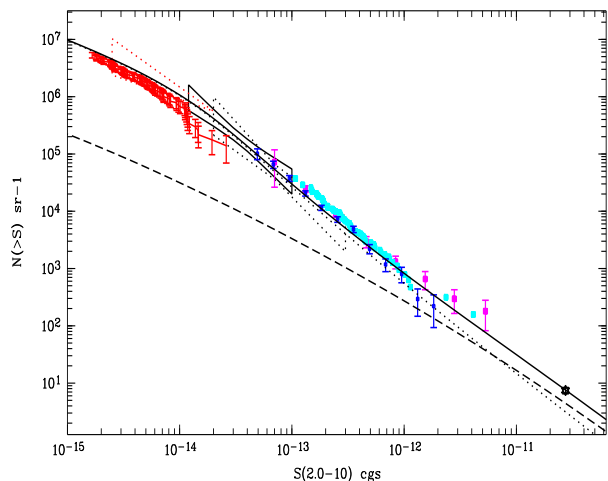


Figure 3. A compilation of the 2–10 keV $\log N$ – $\log S$ from different surveys. Blue dots = BeppoSAX, Giommi et al. 2000; magenta squares = ASCA, Ueda et al. 1999; cyan squares = ASCA, Della Ceca et al. 1999; red error bars = Chandra, Giacconi et al. 2001; black star = HEAO1, Piccinotti et al. 1982; black thick bow tie = the 1σ region delimited by the analysis of BeppoSAX fluctuations, Perri & Giommi 2000; black dot bow tie = the 1σ region delimited by the analysis of ASCA SIS fluctuations, Gendreau et al. 1998; red dot bow tie = Chandra $\log N$ – $\log S$ using eq. 2 of Mushotzky et al. 2000). Thick line = total (AGN+clusters) 2–10 keV counts predicted by the XRB synthesis model; dotted line = AGN only; dashed line = clusters only.

The solid thick line in fig. 2 represents the expectation of the model described in the previous section. This includes both AGN and clusters. The expected number counts relation for cluster of galaxies has been computed assuming an average temperature of 6 keV and the local luminosity function of Piccinotti et al. (1982) with no evolution. The cluster contribution, which is never dominant at the 5–10 keV fluxes sampled by BeppoSAX, is reported only for completeness. We note that a detailed calculation of cluster source counts using more recent estimates for the clusters XLF (Ebeling et al. 1997) provides similar results. The predicted hard X-ray counts are also consistent with the recent XMM-*Newton* observations in the Lockman hole reaching 5–10 keV fluxes about an order of magnitude fainter (Hasinger et al. 2001). The expectation of the same model are also compared with a compilation of number counts in the 2–10 keV band (Fig. 3) from BeppoSAX (Giommi et al. 2000), ASCA (Ueda et al. 1999, Della Ceca et al. 1999) and Chandra (Mushotzky et al. 2000, Giacconi et al. 2001) surveys. A good agreement between model predictions and observations is obtained with the BeppoSAX and ASCA 2–10 keV number counts, and with the Mushotzky et al. (2000) *Chandra* counts while the measurements of Giacconi et al. (2001) are slightly overpredicted.

The key parameter of all the XRB models is the space density of obscured AGN and their absorption distribution. It is customary to adopt a ratio between obscured and unobscured objects consistent with the value measured for samples of nearby (often optically selected) type 2 and type 1 Seyferts galaxies. In the model discussed here such a ratio is not assumed a priori but determined from the XRB fitting procedure and thus it is obviously dependent on the column density adopted to divide absorbed from unabsorbed objects. The ratio between obscured and unobscured AGN is thus about 4.3 if such a value is set to 10^{22} cm $^{-2}$ and about 2.4 for $N_H = 3 \times 10^{22}$ cm $^{-2}$. We stress that such a ratio is independent from optical classification and thus the relative fraction of X-ray obscured AGN in a flux limited survey could be different from the fraction of optically narrow-lined type 2 objects. It is important also to note that the above quoted values for the ratio between obscured and unobscured objects are referred to the entire AGN population responsible for the XRB intensity and that such a number would be recovered only when the full XRB is resolved into single sources. The fraction of objects with a given column density actually included in a survey depends on the flux limit of the survey and on the energy range. Figure 4 shows these fractions as a function of the 0.5–2, 2–10 and 5–10 keV fluxes. The dependence of the fractions on the flux is smoother in the harder bands (see Comastri 2000). As a consequence, 5–10 keV surveys can better probe the real fraction of obscured object going down to fluxes comparatively higher than in the 2–10 keV and 0.5–2 keV bands. As an example at 5–10 keV fluxes of the order of 10^{-13} erg cm $^{-2}$ s $^{-1}$ the fraction of objects in the $\log N_H = 23$ –24 bin is of the order of 25% while is some < 15 % in the 2–10 keV band and negligible in the soft 0.5–2 keV energy range.

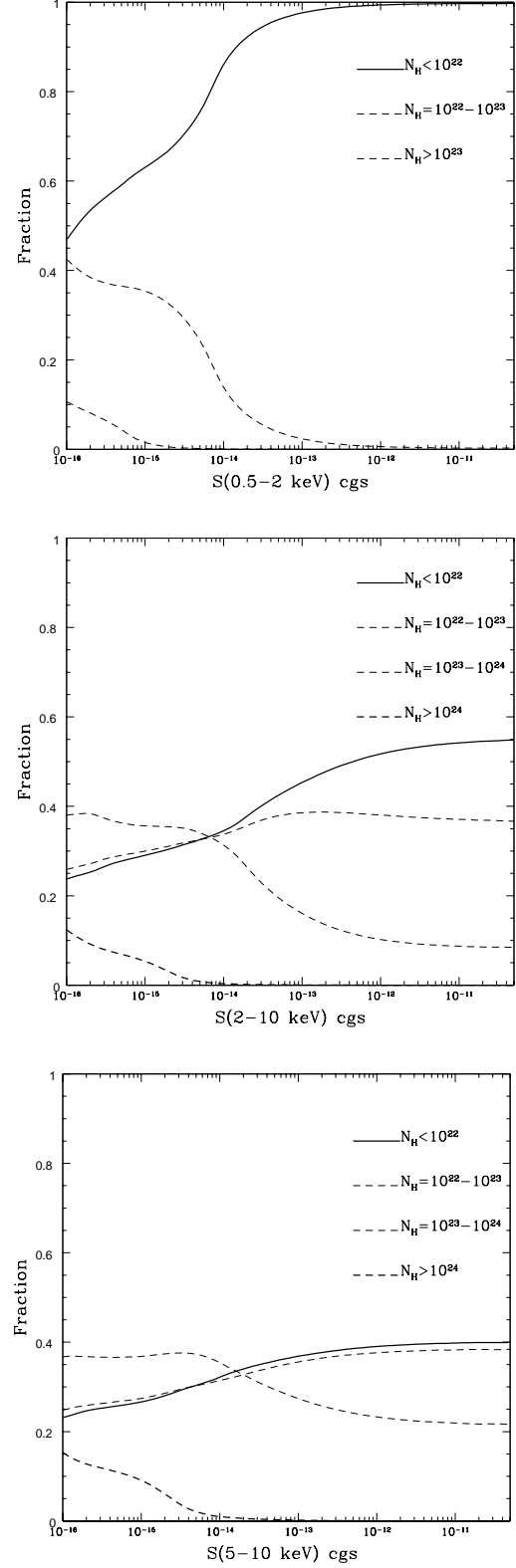


Figure 4. The relative fraction of unobscured (solid line) and obscured sources (dashed lines where the thickness increases for increasing absorption) as a function of the 0.5–2, 2–10 and 5–10 keV flux from top to bottom respectively.

4.1 The luminosity and absorption distribution of obscured AGN

In order to investigate to what extent the present data can be used to constrain the absorption and luminosity distribution of the sources making the hard XRB, additional tests of synthesis models have been carried out. More specifically we have computed 2 models which both reproduce the XRB spectral shape over the 3–100 keV energy range with somewhat “extreme” assumptions on the absorption and luminosity distribution of the obscured sources. In the former case we have maximized the number of obscured Compton thick sources (about a factor 2 with respect to the baseline model), while in the latter a cut-off in the luminosity function of absorbed AGN has been introduced for luminosities greater than 10^{44} erg s⁻¹. These attempts are motivated by both theoretical and observational evidence as described below.

An XRB model dominated by a population of almost Compton thick ($\tau_T \simeq 1$) sources has been worked out by Wilman et al. (2000) based on the suggestion of Fabian (1999) who argued that significant obscuration might be associated with the growth of massive black holes in protogalactic bulges. The Wilman et al. (2000) model predicts a similar contribution from obscured and unobscured objects at about 30 keV. In order to reproduce the XRB spectrum below about 10 keV additional obscuration with an average column of $N_H = 10^{22.75}$ cm⁻² is introduced for 70% of the remaining objects.

We have computed a synthesis model with an absorption distribution dominated by Compton thick sources. The contribution of these sources to the XRB is normalized to that obtained by Wilman et al. (2000, see their figure 1) while the absorption distribution for sources with lower column densities is tuned to keep the overall number of objects in the various N_H classes equal to that of our baseline model and to fit the XRB spectrum.

The 5–10 keV predicted counts are reported in Figure 5 and compared with the observed HELLAS counts and with the baseline model predictions. The y-scale is the product of the integral counts times the flux. In this representation the fluxes contributing most to the XRB are around the peak of the distribution.

The contribution of Compton thick sources is never dominant in the 5–10 keV band, as a consequence, the bright part of the logN–logS is not well reproduced by the model where their contribution is maximized. Even though the uncertainties associated with the hard HELLAS and XMM–Newton counts do not allow to rule out a large number of highly obscured AGN, it is clear that on the basis of present data an N_H distribution peaked at lower column densities has to be preferred.

The evolution of the luminosity function of absorbed sources is assumed to be the same of unobscured one in almost all the XRB synthesis models. The lack of luminous narrow line quasar (type 2 QSO) in optical surveys has lead several authors (see the discussion in Halpern et al. 1998) to conclude that either they are very rare or even do not exist. We checked the importance of high-luminosity highly absorbed AGN by fitting the XRB with a mixture of unabsorbed AGN at all luminosities and low-luminosity absorbed AGN with an approach similar to that described by Gilli et

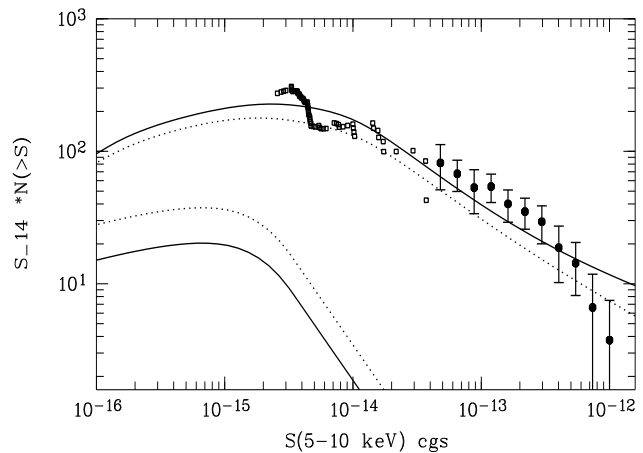


Figure 5. The 5–10 keV HELLAS and XMM–Newton counts are compared with the Compton–thick–dominated model (dotted lines) and with the baseline model (solid lines) predictions. The contribution of Compton thick sources in the two models is also reported.

al. (2001). Here a sharp cut-off in the luminosity function of obscured AGN is introduced for luminosities greater than 10^{44} erg s⁻¹. The shape of the absorption distribution is the same of the baseline model; however, in order to reproduce the XRB spectral intensity, the number of sources in each absorption class has to be increased by 20%. The predicted 5–10 keV counts are reported in Fig. 6 and compared with the observational data and with the baseline model. It is clear that with such a model the HELLAS counts at relatively bright fluxes are severely underestimated since most of the XRB energy density is due to low luminosity AGN emerging only at lower fluxes (Comastri 2000).

5 THE HELLAS AVERAGE SPECTRAL PROPERTIES COMPARED WITH MODEL PREDICTIONS

To evaluate the absorbing column density of the HELLAS sources from the X-ray count ratio, the redshift of the source should be known (assuming that the absorber is at the same redshift of the source, see Fiore et al. 1998). To this purpose we plot $(S-H)/(S+H)$ as a function of redshift (Figure 7) for a subsample of 51 sources with optical spectroscopic identification (La Franca et al. 2001). The dotted lines represent the expectation of unabsorbed power laws with $\alpha_E = 0.8$ and 0.4. The dashed lines represent the expectations of power law absorbed by columns of 10^{23} , $10^{23.5}$ and 10^{24} cm⁻², respectively, *in the source frame*. As expected, the softness ratio of constant column density models strongly increases with the redshift. Many of the identified HELLAS sources have $(S-H)/(S+H)$ inconsistent with that expected from an unabsorbed power law model with $\alpha_E = 0.8$. Substantial absorbing column densities are implied.

Not surprisingly, almost all the sources in the nearby Universe ($z < 0.3$), which are likely to be obscured by column densities $N_H > 10^{22.5-23}$ cm⁻², are narrow line, type

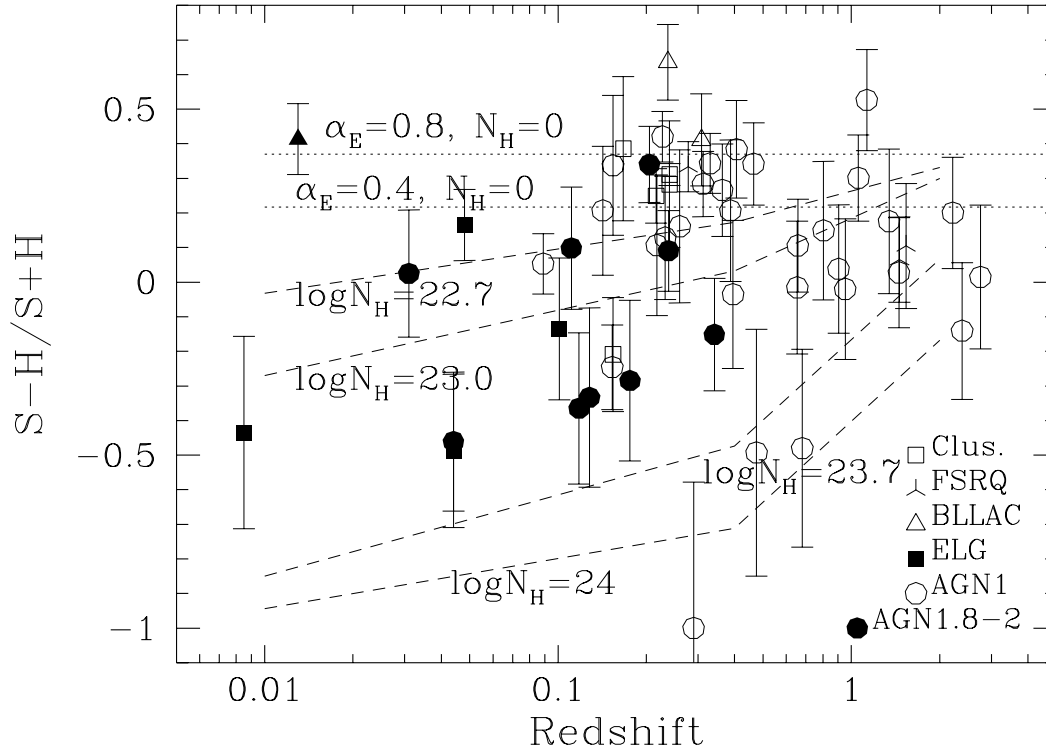


Figure 7. The softness ratio $(S-H)/(S+H)$ as a function of redshift for the identified sources. Different symbols mark identified sources: open circles = broad line, ‘blue’ continuum quasars and Sy1; stars = broad line ‘red’ continuum quasars; filled circles = type 1.8-1.9-2.0 AGN; filled squares = starburst galaxies and LINERS; open triangles = radio loud AGN. The dotted lines show the expected hardness ratio for power law models with $\alpha_E=0.8$ and 0.4 . Dashed lines show the expectation of absorbed power law models (with $\alpha_E = 0.8$ and $\log N_H=24, 23.7, 23.0, 22.7$ from bottom to top) with the absorber at the source redshift.

1.8-2 AGN (Fiore et al. 1999, 2000; La Franca et al. 2001), while broad line AGN are relatively unabsorbed in agreement with popular AGN unification schemes. The situation is different at high redshift where several broad-line AGN appear to have strongly absorbed X-ray spectra. The statistics in the present observations are not good enough to definitely assess this point. XMM-Newton observations may easily confirm or disprove a significant absorbing column in these sources. The presence of highly X-ray obscured quasars with broad optical lines implies a dust-to-gas ratio or a dust composition strongly different from the Galactic one (Maiolino et al. 2001). Alternatively, the X-ray absorber could be much closer to the central source than the Broad Line Region within the dust sublimation radius. This radius depends on the central source luminosity and thus if the X-ray absorbing gas lies at the same distance from the ionizing source, the higher the X-ray luminosity the lower the dust extinction is. Although the nature of X-ray absorption in broad lines blue continuum quasars is not well understood, it is interesting to note that large column of cold gas have been detected in broad absorption line quasars (Gallagher et al. 1999), bright PG quasars (Gallagher et al. 2000) and

high redshift quasars (Elvis et al. 1994; Cappi et al. 1997; Fiore et al. 1998; Yuan et al. 2000; Fabian et al. 2000).

The column density distribution inferred from Fig. 7 is compared with the baseline model predictions in Fig. 8. Given that the 5–10 keV band is not sensitive to column densities below about 10^{23} cm^{-2} , sources with lower column densities are grouped in a single bin. The two BL Lac objects have been neglected in the calculation as this class of objects is not included in the synthesis model. The two boxes correspond to the observed fraction ($\pm 1 \sigma$) of HELLAS sources for each absorption class and cover the flux decade 5×10^{-14} – 5×10^{-13} corresponding to the fluxes of the large majority of the sources in Fig. 7. In order to take into account the relatively large errors in the softness ratio values a source is included in the corresponding N_H class only if its softness ratio value plus one sigma error is below the N_H value indicated by the dashed lines in Fig. 7. According to this prescription there are no sources with column densities greater than 10^{24} cm^{-2} , the corresponding upper limit was obtained assuming that the two objects with a “best fit” column density $> 10^{24} \text{ cm}^{-2}$ are indeed Compton thick. It is important to note that the relatively good agreement

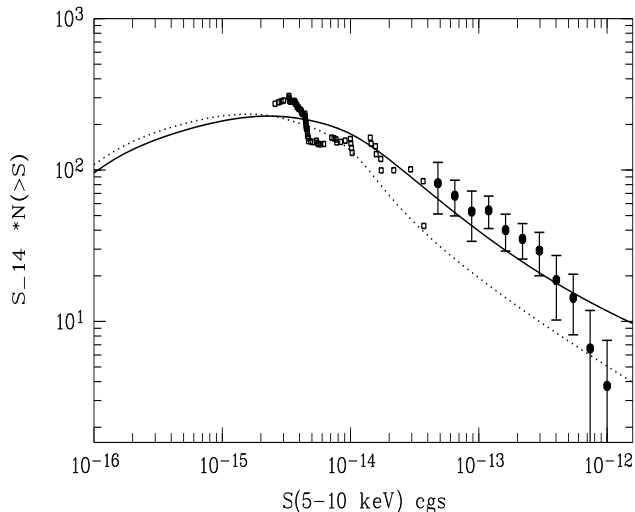


Figure 6. The 5–10 keV HELLAS and XMM–*Newton* counts are compared with the predictions of a model without high luminosity highly obscured objects (dotted line) and with the baseline model.

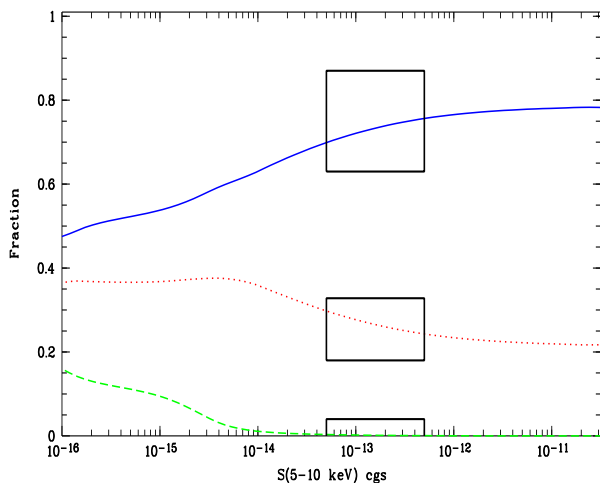


Figure 8. The model predicted fraction of relatively unobscured ($\log N_H < 23$, solid line), highly absorbed ($23 < \log N_H < 24$, dotted line) and Compton Thick ($\log N_H > 24$, dashed line) AGN as a function of the 5–10 keV flux. The boxes corresponds to the fraction of objects in the corresponding N_H classes as computed from the softness ratio vs. redshift diagram of figure 7.

between model predictions and observed N_H distribution is obtained without considering the optical classification.

6 DISCUSSION AND CONCLUSIONS

The HELLAS survey described in the companion paper by Fiore et al. (paper II) provided a statistically well defined

and flux limited sample of 147 hard X-ray selected sources used to estimate the 5–10 keV $\log N$ – $\log S$ and the average X-ray spectral properties of the objects responsible for a significant fraction of the 5–10 keV XRB (from 20 to 30% depending from its normalization; Vecchi et al. 1999, Comastri 2000). The analysis of X-ray colors indicates that HELLAS sources have rather hard spectra, harder than the average spectra of sources in the 0.7–10 keV ASCA surveys (Ueda et al. 1999, Della Ceca et al. 1999). This hardness may be due to substantial absorbing columns. In fact, a large fraction of identified type 1.8–2 AGN and also a few broad line Seyfert 1 galaxies and quasars show softness ratios similar to those expected from power law models reduced at low energy by column densities of $\log N_H = 22$ –24, at the source redshift.

The relatively high number of hard sources discovered by BeppoSAX in the hardest band accessible with imaging instruments makes the HELLAS survey extremely well suited to test AGN synthesis models predictions.

The baseline model described in detail in previous sections is able to reproduce the 5–10 keV counts as observed by BeppoSAX and XMM–*Newton* and is also consistent with the 2–10 keV $\log N$ – $\log S$ as measured by several instruments. The bright tail of the 5–10 keV $\log N$ – $\log S$ as measured by BeppoSAX is best fitted by a model with a significant fraction of highly obscured, high luminosity AGN in good agreement with the findings of Gilli et al. (2001) based on the 2–10 keV counts. A large fraction of Compton thick sources, as envisaged in the model by Wilman et al. (2000) and Fabian (1999), does not adequately reproduce the HELLAS counts, however the presence of a sizeable number of sources with $N_H > 10^{24} \text{ cm}^{-2}$ cannot be strongly ruled out based on the 5–10 keV counts. Imaging observations at energies greater than about 20 keV, such as those planned with the Energetic X-ray Imaging Survey Telescope (EXIST, Grindlay 2000), are required to test such possibility.

The baseline model can be considered as the simplest version of AGN synthesis model. In fact the absorption distribution adopted to fit the hard XRB spectrum and the source counts in different energy ranges are independent from source redshift and luminosity. Moreover, such a distribution is also in good agreement with that derived from observations of nearby AGN (Risaliti et al. 1999).

The optical identification of a sizeable number of HELLAS sources allowed to further constrain the absorption distribution, for column densities lower than $\simeq 10^{24} \text{ cm}^{-2}$, over a large range of redshifts and luminosities. The most important result concerns the optical appearance of X-ray obscured AGN as a function of redshift. In the local Universe absorbed objects are almost always associated with narrow line optical spectra while at high redshifts ($z > 0.3$) the presence of X-ray obscured sources with broad optical lines strongly suggest a decoupling between the X-ray and optical classification. We note that such a result does not affect the AGN synthesis model which is entirely based on the X-ray properties. It is concluded that, as far as the present observational constraints are concerned, there is no need for a significant revision of the baseline model assumptions which turn out to adequately reproduce both the XRB spectrum and the source counts.

The optical identification of a sizeable sample of hard X-ray selected sources from *Chandra* and XMM–*Newton* surveys coupled with high quality X-ray spectroscopy, es-

pecially for high redshift quasars, will provide new insights on the nature and the physics of the sources of the XRB.

Acknowledgements

We thank the BeppoSAX SDC, SOC and OCC teams for the successful operation of the satellite and preliminary data reduction and screening. We also thank R. Maiolino, S. Molendi, F. Pompilio, M. Perri, M. Salvati and G. Zamorani for useful discussions and G. Hasinger for providing the XMM-Newton counts in the 5–10 keV band in a computer readable format. This research has been partially supported by ASI contract ARS-99-75 and MURST grants Cofin-98-032 and Cofin00-02-36.

REFERENCES

- Akiyama, M. et al. 2000, ApJ 532, 700
 Almaini, O., et al. 1996, MNRAS 282, 295
 Boyle, B. et al. 1993, MNRAS, 260, 49
 Boyle, B. et al. 1994, MNRAS, 271, 639
 Boyle, B. et al. 1998, MNRAS, 296, 1
 Cagnoni, I., Della Ceca, R., Maccacaro, T. 1998, ApJ, 493, 54
 Cappi, M., Matsuoka, M., Comastri, A., Brinkmann, W., Elvis, M., Palumbo, G.G.C., Vignali, C., 1997, ApJ 478, 492
 Ciliegi P., Vignali C., Comastri A., et al. in preparation (paper VI)
 Comastri, A. Setti, G., Zamorani, G., Hasinger, G. 1995, A&A, 296, 1
 Comastri, A., 2000, Astr. Lett. and Comm., in press, proceedings of the conference “X-ray Astronomy ’999, Stellar Endpoints, AGN and the Diffuse Background” (astro-ph/0003437)
 Della Ceca, R., Castelli, G., Braitto, V., Cagnoni, I., Maccacaro, T. 1999 ApJ, 524, 674
 Ebeling H., Edge A.C., Fabian A.C., Allen S.W., Crawford C.S., Böhringer H. 1997, ApJ 479, L101
 Elvis, M., Fiore, F., Wilkes, B.J., McDowell, J.C., Bechtold, J., 1994, ApJ 422, 60
 Fabian, A.C., 1999, MNRAS 308, L39
 Fabian A.C., Celotti A., Iwasawa K., McMahon R.G., Carilli C.L., Brandt W.N., Ghisellini G., Hook I.M., 2000, MNRAS in press (astro-ph/0011566)
 Fiore, F., Elvis, M., Giommi, P., Padovani, P., 1998, ApJ, 492, 79
 Fiore, F. et al. 1999, MNRAS, 306, L55 (paper I)
 Fiore, F. et al. 2000, Astr. Lett. and Comm. in press, proceedings of the Bologna meeting “X-ray Astronomy ’999, Stellar Endpoints, AGN and the Diffuse Background” astro-ph/0007118
 Fiore F., Giommi P., Vignali C., et al. 2001, MNRAS, submitted (paper II)
 Gallagher S.C., Brandt W.N., Sambruna R.M., Mathur S., Yamasaki N., 1999, ApJ 519, 549
 Gallagher S.C., Brandt W.N., Laor A., Elvis M., Mathur S., Wills B.J., Iyomoto N. 2000 ApJ in press, (astro-ph/0007384)
 Gendreau K.C., Mushotzky R.F., Fabian A.C., et al. 1995, PASJ 47, L5
 Gendreau K.C., Barcons X., Fabian A.C., 1998, MNRAS 297, 41
 Georgantopoulos, I., et al. 1997, MNRAS, 291, 203
 Giacconi R., Rosati P., Tozzi P., et al. 2001, ApJ, in press, astro-ph/0007240
 Gilli R., Risaliti G., Salvati M., 1999, A&A 347, 424
 Gilli R., Salvati M., Hasinger G., 2001, A&A 366, 407
 Giommi, P., Perri M., Fiore F., 2000, A&A 362, 799
 Grindlay J., and the EXIST Science Working Group, AAS Bulletin 32, No. 3, 20.04
 Halpern, J.P., Eracleous, M., Forster, K. 1998, ApJ, 501, 103
 Hasinger, G. et al. 1998, A&A, 329, 482
 Hasinger G., Altieri B., Arnaud M., et al. 2001, A&A, 365, L45
 La Franca F., Fiore F., Vignali C., Comastri A., Pompilio F., 2000 in Proceedings of the conference : “The New Era of Wide-Field Astronomy” held in Preston (UK), August 2000 (astro-ph/0011008)
 La Franca F., Fiore F., Matt G., et al., in preparation (paper V)
 Lehmann, I. et al. 2000, A&A 354, 35
 Madau P., Ghisellini G., Fabian A.C., 1994, MNRAS 270, L17
 Maiolino R., Marconi A., Salvati M., et al. 2001, A&A 365, 28
 Marshall, F.E., Boldt, E.A., Holt, S.S., Miller, R.B., Mushotzky, R.F., Rose, L.A., Rothschild, R.E., Serlemitsos, P.J., 1980, ApJ 235, 4
 Matt G., Pompilio F., La Franca F., 1999, New Astron. 4, 191
 Miyaji, T., Hasinger, G., Schmidt, M. 2000, A&A, 353, 25
 Mushotzky R.F., Cowie L.L., Barger A.J., Arnaud K.A., 2000, Nature 404, 459
 Perri, M., Giommi, P., 2000, A&A 362, L57
 Piccinotti G., Mushotzky R.F., Boldt E.A., et al. 1982, ApJ 253, 485
 Pompilio F., La Franca, F., Matt, G., 2000, A&A, 353, 440
 Risaliti G., Maiolino R., Salvati M., 1999, ApJ 522, 157
 Schmidt, M. et al. 1998, A&A 329 495
 Setti, G., Woltjer, L., 1989, A&A, 224, L21
 Ueda, Y. et al. 1998, Nature, 391, 866
 Ueda, Y. et al. 1999, ApJL, 524, L11
 Vecchi, A., Molendi, S. Guainazzi, M., Parmar, A., Fiore F., 1999, A&A, 349, L73
 Vignali, C., Comastri, A., Fiore, F., La Franca F., 2001, A&A submitted (paper IV)
 Wilman, R.J., Fabian, A.C., 1999, MNRAS, 309, 862
 Wilman, R.J., Fabian, A.C., Nulsen, P.E.J., 2000, MNRAS 319, 583
 Yuan W., Matsuoka M., Wang T., Ueno S., Kubo H., Mihara T., 2000 ApJ 545, 625